Article:
Parody Martin, A. and Marshall, M.B. (2026) Measurement of grit wear in abrasive c-BN electroplated tipped blades for gas turbines applications. Wear, 589. 206538. ISSN: 0043-1648

https://doi.org/10.1016/j.wear.2026.206538

Measurement of grit wear in abrasive c-BN electroplated tipped blades for gas turbine applications

A. Parody Martin[a,*], M.B. Marshall[b]

[a]Department of Engineering, Universidad Loyola Andalucía, Av. de las Universidades, 2, Dos Hermanas, Sevilla, 41704, Dos Hermanas, Sevilla Spain
[b]Department of Mechanical, Aerospace and Civil Engineering, The University of Sheffield, Mappin Street, Sheffield S1 3JD, UK

ARTICLE INFO

Keywords:
abrasive electroplated coating
wear measurement
grit wear mechanisms
surface topography
incursion test
c-BN
abradable ceramic coating

ABSTRACT

The increasing use of ceramic abradable seal systems in the High-Pressure Turbine section of gas turbines, aimed at improving efficiency and reducing fuel consumption, introduces new challenges in performance evaluation. This work proposes a standard method to quantify wear on c-BN electroplated tipped blades, which function as abrasive coatings on rotor blades. The approach relies on 3D metrology scanner to capture surface data of the blade and converting them into measurable parameters that allow for consistent comparison between blades from rig testing. Key metrics include grit density, the volume occupied by abrasive particles, and the corresponding void volume and void density resulting from wear. An additional parameter is proposed to account for debris accumulation and its effect on the proposed wear-related metrics. The results demonstrate consistent trends across the proposed parameters, both in pristine and tested blades, regardless of their initial grit density as well as with grit wear patterns. The proposed Positive Volume Variation (PVV) and Grit Density Variation (GDV) metrics exhibited a strong mutual correlation (r = 0.950), a result supported by their shared underlying physical basis. In contrast, the Mean Height Variation (MHV), typically applied to bare blades, demonstrated weaker correlations with both PVV (r = 0.893) and GDV (r = 0.745).

1. Introduction

In gas turbine engines, the clearance between blade tips and the casing is a major source of efficiency loss [1, 2]. Gas escaping through this gap bypasses the aerofoils, reducing the effectiveness of energy transfer between the fluid and the rotor. Consequently, the engine must burn more fuel to compensate for these parasitic losses and maintain thrust.

Abradable seal systems are essential in both the compressor and turbine stages to minimise this tip clearance between rotating blades and stationary components. By allowing controlled contact during engine operation, these systems enable tighter tolerances than would otherwise be possible. In compressor stages, these systems use metal-based abradables that allow bare metal-based blades to cut grooves into them during the engine's first run, establishing the minimum clearance needed for regular operation. This sacrificial contact prevents damage to the rotor while ensuring near-zero clearance.

In contrast, the turbine section operates at much higher temperatures and therefore relies on ceramic-based abradable coatings like Yttria-Stabilised Zirconia (YSZ) or Magnesium Aluminate Spinel (MAS), which retain their structural integrity under extreme heat but are significantly harder than metal-based alternatives. To cut effectively into these tough coatings and avoid blade damage during contact, turbine blades must be tipped with abrasive materials where cubic boron nitride (c-BN) embedded in a MCrAlY metallic matrix and deposited via electroplating is the standard solution employed in the High Pressure turbine (HPT).

*Corresponding author
aparody@uloyola.es (A. Parody Martin)
ORCID(s): 0009-0003-8937-6206 (A. Parody Martin)

Given the demanding conditions and material complexity, assessing the performance of these abrasive-tipped blades requires comprehensive testing. To support this, a new analytical procedure developed in MATLAB is introduced to evaluate electroplated tipped blades used in abradable incursion testing [3] for assessing abradable seal performance. The two features that are sought to be quantified through this technique are the blades remaining cutting capability as well as the blade wear prior to failure. The performance of abrasive blades is to some degree probabilistic as they are a composite material and need more than one test repetition at specific test conditions to be characterised. Therefore, the high volume of tests required has motivated the development of a computer-aided tool designed to streamline analysis and ensure repeatable results.

Previous research on abrasive-tipped blades has frequently employed analysis techniques originally developed for bare blades. These methods primarily rely on quantifying changes in overall blade height, weight, or volume, alongside characterizing the geometry and visual appearance of the abradable groove [4, 5, 6, 7, 8]. Regarding height quantification, the Mean Height Variation (MHV) is the standard metric [8, 9, 10, 11]; it averages height differences across the blade width. Furthermore, these measurements can be normalised to derive efficiency ratios: the Incursion Depth Ratio (IDR) relates blade height loss to the total incursion depth, while the Incursion Quality Ratio (IQR) correlates blade weight loss with the mass removed from the abradable coating [8, 12].

Using the overall weight or volume difference as an indicator for the performance of bare blades during a test is appropriate as the material is homogeneous and their behaviour can be simplified as a binary phenomenon. In this context, an increase in weight, volume, or mean height is

attributable to material adhesion from the abradable (generally metal based) to the blade tip. Conversely, a reduction in these parameters signifies wear, typically resulting from rough contact where the blade tip reaches its melting point and erodes.

However, for abrasive-tipped blades, this behaviour is non-binary, rendering net weight or volume change a poor indicator of performance. Multiple competing phenomena may occur simultaneously, introducing variations that generally decrease, but occasionally increase, the total volume. While material adhesion is the sole mechanism adding volume, several mechanisms simultaneously remove material from the abrasive coating [4, 5, 6, 7]:

- Grit fracture: occurs when a portion of the grit breaks off, while the remainder of the particle stays attached to the bonding system. It renews fresh and sharp edges. According to the extent of the remaining portion and the remaining cutting capability, fracture wear can be split into microfracture and macrofracture.
- Attritious wear: involves dulling of the abrasive grains through the formation of rounded edges and flat spots, driven by both physical and chemical mechanisms.
- Grit pull-out: occurs when abrasive grains are completely dislodged from the attachment layer when the bonding strength at the grit-matrix interface is exceeded, leaving a void crater behind.

Furthermore, the height metric typically employed for bare blades relies on the averaged height of the blade's 2D projection [9, 10]. Since bare blade wear is generally homogeneous across the blade thickness, this projected mean height remains a robust metric. However, for abrasive-tipped blades, wear is localised on individual grits distributed across the blade thickness. Consequently, relying on a 2D projection is problematic. The grits positioned at the leading edge effectively mask the wear of the grits situated behind them, obscuring the true extent of the damage.

Similarly, the length or depth of the groove generated on the abradable sample has been employed as a comparative indicator [5]. While appropriate for bare blades, where wear directly impacts blade height and groove geometry [13, 9, 10], this approach is insufficient for abrasive tips. Considering the typical size of c-BN abrasive grits (60/80 US mesh) used in aero-engines [14], depth variations caused by grit fracture are on the order of tens of microns. Such subtle variations are often masked by the dynamic response (vibration) of the test rig, making them difficult to distinguish from noise. Additionally, rig-specific dynamics affect track length, complicating cross-comparison [10]. Indeed, for abrasive-tipped blades, wear would likely only become discernible via this method once the blade has failed catastrophically, providing no insight into performance during its functional lifetime [5].

As there is not a standard approach for assessing wear on gas turbine abrasive tipped blades, the closest analogies that might be applied are the methodologies employed in grinding wheels. Wear in conventional grinding wheels, manufactured by a cold-press method, is evaluated as the ratio between the volume of the removed workpiece material and either the wheel volume loss or the reduction of the wheel radial length [15, 16]. However, these types of grinding wheels suffer from dressing in which both grits and matrix get removed to unveil new grits underneath and, therefore, make the volume ratio approach suitable for the application, but not applicable to gas turbine abrasive electroplated tipped blades which comprise a single abrasive layer. When it comes to superabrasive electroplated grinding wheels, which now consist of a single layer of protruding abrasive grits, grit count and power monitoring techniques are employed instead [15, 17, 16].

One notable exception came during the development of new abrasive-tipped blade solutions at the University of Cambridge, which utilised electroplated grinding wheel grit counting technique [18]. This manual method involves quantifying grit microfracture, macrofracture, and pull-outs on the abrasive coating to correlate these with blade performance. While successful, the approach is limited by small sampling areas and the lack of computer-aided tools, rendering it inefficient for analyzing large test batches or repeated trials, a crucial capability when characterizing the stochastic nature of abrasive-tipped coatings.

Given the gap in research with regards to the analysis of abrasive tipped blades employed in abradable incursion tests, this paper aims to develop a new MATLAB-based analytical methodology to assess blade wear, prior to failure, for its later implementation in blade performance analysis.

2. Methodology

To generate controlled damage on the electroplated tipped blades, intended for subsequent analysis using the methodologies later outlined in this section, the same testing procedure employed in earlier research on the scaled test rig at the University of Sheffield has been followed [19, 20, 13, 10]. A detailed description of this rig can be found in previous work [19], and an illustration is provided in Figure 1. The setup includes a grinding spindle that holds a 2 mm thick test blade, as the one shown in Figure 2a, along with a dummy blade for balance. The abradable specimen, seen in 2b, is positioned on a z-axis microscope stage located beneath the blade.

Prior to testing, the microscope stage is adjusted so that the blade and abradable surface are just in contact. The test begins by retracting the abradable, spinning up the spindle to the target speed, and then advancing the abradable toward the rotating blade at a controlled incursion rate using the microscope stage. This setup results in intermittent, high-speed contacts between the blade and the abradable surface.

The six test blades used to develop the damage quantification tools in this study are c-BN electroplated tipped CMSX-4 Nickel-based superalloy blades (Figure 2a), whose

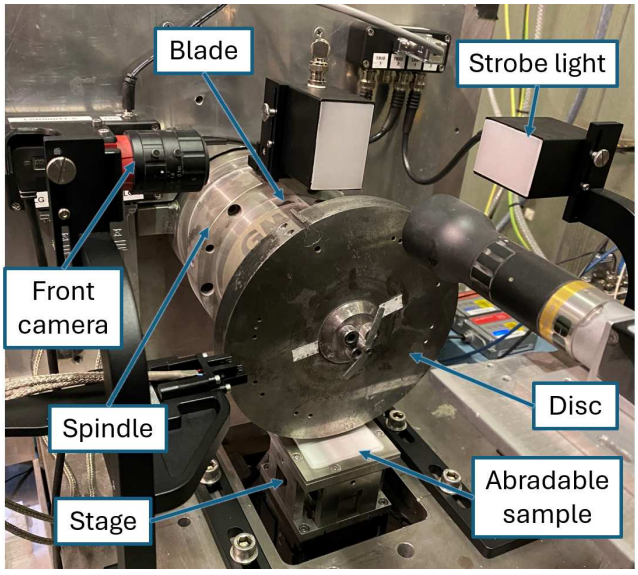

Figure 1: Scaled abradable test rig at the University of Sheffield.

abrasive coating is commercially available from Praxair Surface Technology under the name of Tribomet TBT429 [21]. To ensure experimental consistency, all blades were sourced from a single manufacturing batch produced under identical parameters. The differences in grit density, visible in Figure 3, are attributed to the stochastic nature of the co-deposition process. Despite this variability, all blade coatings fall within established process control ranges.

The abradable material to be tested against is Magnesia Alumina Spinel (MAS), seen in Figure 2b, but a series of intermediate layers must be sprayed between this and the substrate to ensure a good adherence and avoid delamination [22, 23, 24]. The substrate is an 80x80x3mm plate made of 316 stainless steel. On top of the substrate, a 150-micron-thick metallic layer of CoNiCrAlY is sprayed to act as a bond-coat with the later ceramic ones. Then, an interlayer 7% Yttria-Stabilised Zirconia (YSZ) with a thickness of 200 microns is sprayed over the bond-coat to gradually bridge the difference in thermal expansion coefficient between the substrate and the final MAS layer, which is sprayed on top with a thickness of 800 μm. The nominal hardness of the MAS layers deposited on the samples used in this study is 63 ± 1.197 HR15N.

The testing procedure replicates the incursion parameters from the standard Rolls-Royce Running-In and Handling (RiH) manoeuvre for turbine sections [14], but performed at room temperature. These incursion parameters included a blade tip speed of 200 m/s, an incursion rate of 0.3 μm/pass, a total incursion depth of 500 μm.

The proposed analysing methodology diagram is illustrated in Figure 4. Firstly, it consists of extracting the surface morphology from the abrasive coating of the blade prior of after being tested with an optical 3D metrology scanner. The extracted data is then discretised into a cloud of points that can be loaded into a numeric computing platform, MATLAB in this case, for its normalisation and later post-processing. The post-processing allow creating measurable parameters that can be decoupled from the measured area, making them directly comparable to other area sizes, the same blade once tested or to different blades. These measurable parameters facilitate the comparison of the wear that blades suffer at different test conditions.

The phases in which the proposed process is divided are presented as: data extraction, normalization of the extracted data, and post processing of the data to construct measurable parameters. Every step is broken down in this section, complemented with examples with the aim of the tool validation.

2.1. Data extraction

Blade surface data is extracted using the Bruker Alicona InfiniteFocusSL 3D measuring instrument and processed with Alicona IF-MeasureSuite. The system captures a high-resolution 2D image, as illustrated in Figure 5a, and a 3D point cloud, as the one shown in Figure 5b. A blade is mounted on a custom holder, and the measurement volume is captured with a horizontal and a vertical resolution of 20 μm and 500 nm respectively. The captured surface comprises approximately 50 million data points uniformly distributed (in a horizontal plane) across a 40 mm^2 area. The data is then processed in MATLAB, where coordinate matrices are constructed for further analysis.

2.2. Data normalisation

To ensure consistency across different blade measurements, the point cloud is normalised through rotation, centering, and tilt correction. Rotation aligns the blade so that its top and bottom edges become parallel to the horizontal axis and the side edges to the vertical axis. Due to the irregular nature of the boundaries of electroplated coatings on thin blades, lines of best fit were generated using the least squares method, and calculating the rotation angle relative to the native coordinate system, which is then applied in reverse to the dataset.

Centering is performed by detecting the blade's boundary points along all edges. The midpoint between the averaged edge values is then used to define the blade's central reference position, ensuring a uniform coordinate system across all samples.

Tilt correction compensates the misalignment of the coating surface with the horizontal plane due to the blade placing on the measuring instrument. Two gradients are calculated along the x and y axes by comparing the average height of all points in designated regions at both ends of the blade in each direction. These gradients are then subtracted from the z coordinates to level the surface, ensuring the blade surface is parallel to the horizontal plane, ending in a normalised blade surface as illustrated in Figure 5b.

Defining the abrasive coating's matrix roughness is essential for the two analysis approaches that are presented next. The matrix roughness is characterised by the arithmetic mean height (Sa), the average maximum peak height (Sp), and the average maximum valley depth (Sv). These parameters are calculated from a set of squared sampling areas

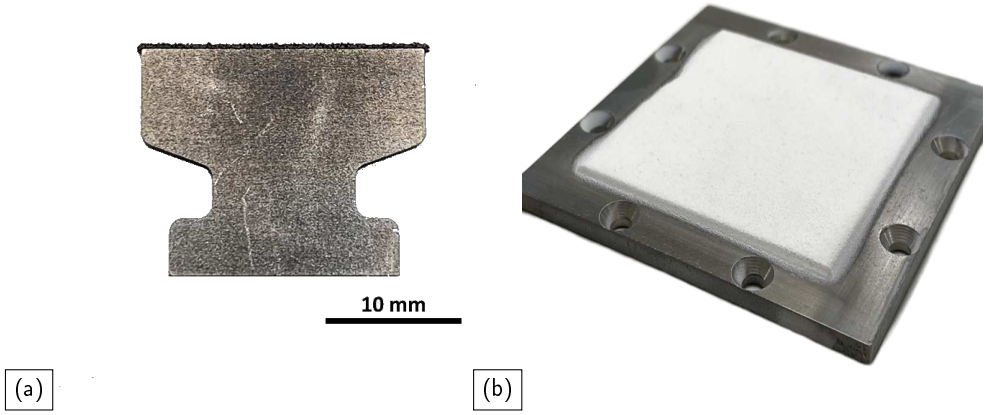

Figure 2: Example of (a) a Tribomet TBT 427 tipped CMSX-4 Nickel-based superalloy blade and (b) a ceramic Magnesia Alumina Spinel abradable sample.

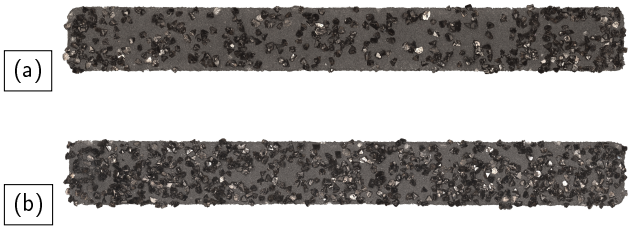

Figure 3: Example of (a) a low-grit-density blade and a (b) high-grit-density blade manufactured under the same paremeters.

manually selected from the matrix, ensuring they contain only points that correspond to the matrix and not to the grits. The mean height (Sa) is determined as the average of all sampled points, while Sp and Sv are calculated from the highest and lowest values of these areas, respectively.

To standardise the data, the z coordinates of all points are normalised by subtracting Sa, setting the mean matrix height to zero, and this establishing a reference plane.

2.3. Data post-processing

Once the blade surface is normalised, two methods are used to assess the blade's wear:

- Volume quantification of the abrasive coating relative to the outlined reference plane
- Identification of surface features such as grits and voids/craters from the extracted point cloud.

2.3.1. Volume evaluation

Prior to defining the methodology for the volume calculation, a statistical analysis can be done from the raw coordinates of the points which is directly correlated to the volume as it is later introduced. The cutting capability of a blade can be related to the percentage of points whose height is above the matrix level. A higher percentage of these points indicates a higher cutting capability of a blade as there are more grits sticking out of the matrix. As the matrix level has been set to zero and the roughness of the matrix is known, positive values over Sp denote the existence of protruding grits as observed in Figure 6 where the two untested blades from Figure 3 with visually different grit density are presented. On the other hand, negative values below Sv indicate the presence of voids as it is observed from the negative values of point height in Figure 5b, which are normally generated during the test, although they can appear during the manufacturing process also due to the poor anchoring of highly protruding grits.

Regarding the blade test condition, the percentage distribution of point heights is associated with the remaining cutting capability of a blade. An untested blade may present points whose height is large as it comes from protruding grits and would be reduced when tested due to their wear or failure as Figure 6 illustrates for the high-grit-density blade previously visualised in Figure 3. Although the most protruding grits are the most likely to be worn out first, this effect will not exclusively happen to them. Therefore, points with larger heights always transition to smaller heights when tested.

Likewise, there is a direct relationship between voids and the percentage of points whose height is negative and below Sv. As the appearance of voids occurs when blades are tested, points with positive height coming from the presence of grits in untested blades transition to negative values when voids are generated during the test, increasing the percentage of negative heights as observed in Figure 6.

In addition, the fracture of grits at the bonding level, either by a sudden macrofracture or a continuous microfracture process that exhaust the grit cutting capability, can also be identified from this analysis. This can be inferred from the increase in the percentage of points with heights between Sv

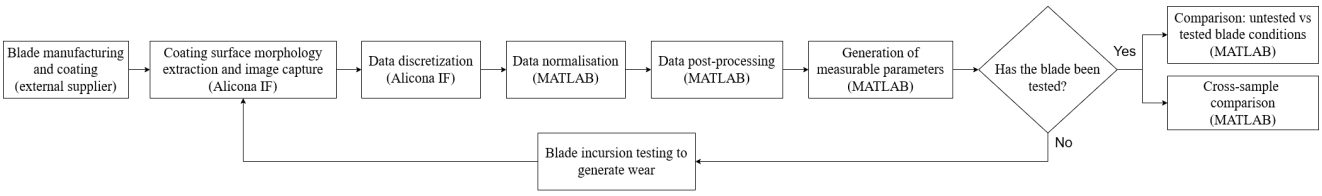

Figure 4: Flowchart of the proposed methodology for blade wear evaluation.

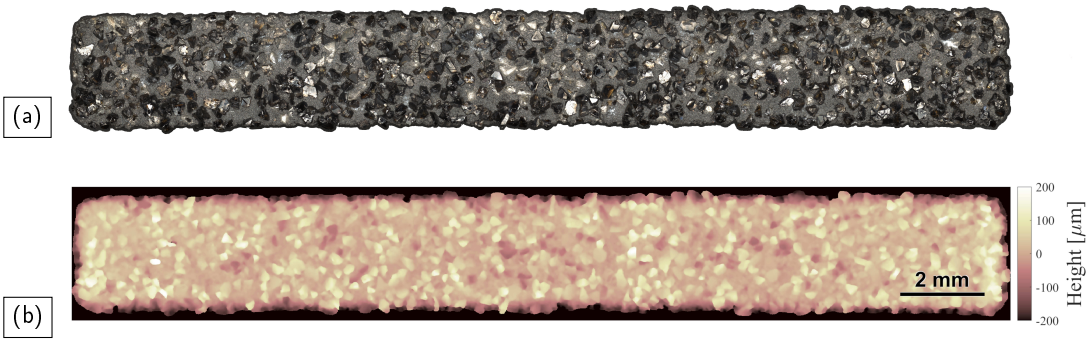

Figure 5: Example of (a) a blade image and (b) the corresponding extracted surface data after normalisation.

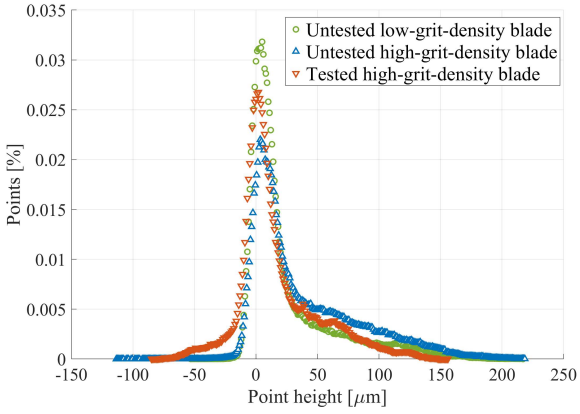

Figure 6: Comparison of point height distributions for the untested low-grit-density blade versus the high-grit-density blade in both tested and untested conditions.

and Sp when comparing the untested and tested blades. This means that technically, there is still a grit anchored to the matrix but its cutting capability is zero as it does not protrude beyond the matrix.

Although the distribution of the heights of the measured points allows the grit and void distribution on a blade to be understood, it is not comparable between blades as the number of points varies from one to another. As the points horizontal position is known, the volume enclosed between the surface and the already defined and zeroed matrix can be calculated for a given area by using the trapezoidal integration rule. As the point mesh is uniform and equidistant for each in-plane axis, the differential volume enclosed between the surface at that point and the matrix level can be calculated by multiplying the point height by the two horizontal constant distances, in both x and y axis, between points. The total volume is then calculated by adding the differential volumes all together. As introduced with the grit height distribution, only volumes where only volumes where the points whose height is either positive or negative can be separately added. In this case, volumes, either positive, negative or total, are independent of the number of points for a given area.

As the horizontal distance between points is constant, the volume differentials follow exactly the same distribution as that of the point heights for a given blade and area. Whereas the volume above the matrix level describes the remaining cutting capability on a blade, the volume below the matrix level represents the voids generated when tested (or manufacturing defects). To enable comparison between different blades, either the analysed area must be the same, or the volume parameters should be normalised by area, making the assessment independent of the sampled region.

Having a single normalised parameter instead of a distribution allows a batch of blades or the variation over the surface of a single blade when tested to be directly compared. In addition, it also allows different areas of the same blades to be compared, which is of particular use in stepped tests where different areas of the blade come into contact with a step-shaped abradable sample at different times during the same incursion test. More details of stepped tests can be found in [20].

2.3.2. Feature detection

The second approach for evaluating the cutting capability and wear produced on a blade as a product of being tested consists of directly counting active grits, voids and other

Figure 7: Portion of a blade showing the non-uniformity between grits in terms of colour and shapes.

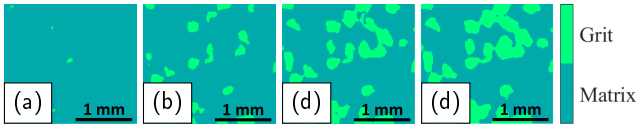

Figure 8: Grit detection process for a 1.8×1.8 mm area at (a) 5%, (b) 35%, (c) 65%, and (d) 100% of the process.

features. Although this seems a simple and straightforward way to assess a blade, the challenge is to computerise the process of identifying them. The high reflectivity, different colours and angles of the multiple grit faces as well as the irregularity of shapes between grits, as shown in Figure 7 make visual recognition extremely challenging. Because of this, a dimensional procedure is developed for the blade feature recognition.

The method for recognising active grits involves incrementally sweeping through the positive height range, starting from the highest point down to the matrix level. Prior to the sweep, two matrices, matching the dimensions of the sampled surface matrix, are initialised:

- Height Boolean Matrix: This matrix is reset at each iteration to indicate which points in the sampled surface matrix are above the current sweep level (*true*) and which are below (*false*).
- Grit identifier Matrix: This matrix stores unique identifiers for each detected grit, assigning the identifier to the corresponding position in the sampled surface matrix.

The process begins at the highest point of the sampled surface, typically detecting a single point. As shown in Figure 8, with each subsequent sweep, previously identified grits expand in cross-sectional area, and new grits may emerge. Before assigning new identifiers, the method detects the spread of existing grits with consecutive sweeps by checking any new (*true*) values adjacent to already existing grits in the Height Boolean Matrix; if so, these points are incorporated into the existing grit with its respective identifier. Points not adjacent to any identified grit are assigned new unique identifiers as represented in Figure 9. This procedure continues iteratively until the sweep reaches the matrix level.

The sweep thickness must be small enough to prevent two adjacent grits in contact from being identified as a single grit, yet large enough to avoid detecting multiple separate cross-sectional areas from the same grit. According

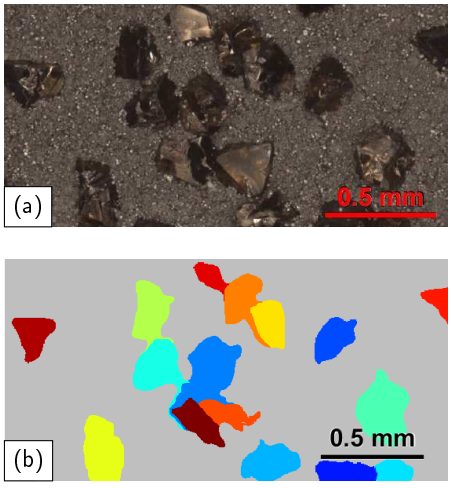

Figure 9: Example of grits active detected by the tool: (a) image of the grits on a TBT429 blade and (b) MATLAB matrix of what is detected as active grits where a different colour is assigned to each grit identifier.

to literature, the Sz peak-to-valley height of 60 grit size c-BN abrasive grits has been reported to range from 10 μm in pristine condition to approximately 3 μm after wear [15].

Therefore, a preliminary sensitivity analysis was conducted on 2 mm^2 regions across a total of 6 distinct samples, selected from both low- and high-grit-density blades. The sweep thickness was varied from the minimum grit size (180 μm) down to 10 μm in 10 μm steps. The analysis revealed that the number of identified grits stabilised at a sweep thickness of 30 μm. Furthermore, visual confirmation ensured that no individual grit was assigned multiple identifiers at this setting, as observed in Figure 9b.

The sweeps are carried out until the matrix level is reached, more exactly, when the double of the Sp value of the matrix is reached. Any point below twice the Sp value and above the matrix level is not considered an active grit, as it assumed not to contribute to cutting. This implies that the projected area of the grits (Figure 9b) does not exactly match the real projected area (Figure 9a). However, this discrepancy serves to exclude localised matrix elevations, caused by grit embedment during the electroplating process, from being identified as grits. Finally, the number of active grits can be divided by the sampled area to obtain the grit density.

The main advantage of this approach is that the outcome provides the number of the grits which is an intelligible

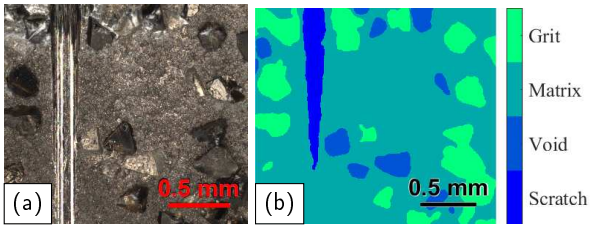

Figure 10: Example of the features detected by the tool: (a) image of region of a TBT429 blade and (b) MATLAB matrix of the detected features.

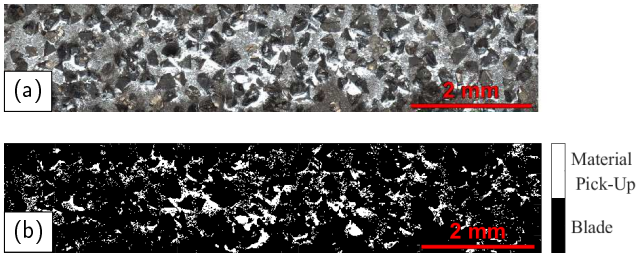

Figure 11: Example of material pick-up detected by the tool: (a) image of a TBT429 blade with MAS material adhered to it and (b) MATLAB matrix of the detected material.

parameter. However, there is a difference between having a given number of grits that were just deposited and protruding significantly, as opposed to having the same number, but where the grits already suffered from wear, and whose maximum height is closer to the matrix bonding level.

Likewise, an analogous procedure is employed for detecting voids, but sweeping the negative heights from the lowest point to the matrix level. In this case, the closing height is twice the value of Sv. If the aspect ratio of a void is significantly out of the range of general c-BN aspect ratios, it is recognised as a scratch on the matrix produced by the absence of grit in that region. Figure 10 illustrate the features recognised from a TBT429 tipped blade by using this method.

2.3.3. Material pick-up

As noted, tested abrasive tipped blades sometimes suffer from material pick up where material from the abradable sample becomes trapped between the abrasive grits of the blades. This phenomenon, when it occurs, may affect the measurements of the two proposed methodologies. Although it is not possible to isolate the adhered material to calculate its volume, an approach is introduced to estimate the degree of material adhesion a blade exhibits after being tested, and to provided contextual data when assessing the two outlined approaches.

The approach is based on the optical recognition of the bright white MAS material trapped on TBT 429 blades, which aside from this are mainly dominated by grey and dark colours, making the MAS material distinguishable. The sampled area is converted from RGB color model into greyscale by following the Equation 1, where I_{Grey} ranges from 0 to 1 [25].

$$I_{\text{Grey}} = 0.2989 \cdot I_{\text{RGB-Red}} + 0.5870 \cdot I_{\text{RGB-Green}} + 0.1140 \cdot I_{\text{RGB-Blue}} \quad (1)$$

As shown in Figure 11, any pixel with a greyscale intensity above a defined threshold is classified as MAS material pick-up. The pick-up ratio is then calculated by dividing the number of pixels above this threshold by the total number of pixels in the area. The threshold is selected to detect the presence of trapped MAS material while minimising false

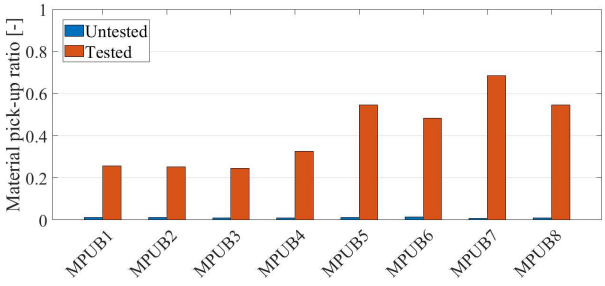

Figure 12: Comparison of the apparent material pick-up for a set of eight blades before and after being tested.

detection caused by grits that appear bright due to light reflection.

A preliminary sensitivity analysis was conducted using dedicated training data to determine an appropriate greyscale threshold for detecting material pick-up on the blades. The objective was to reliably capture material adhered to the tested blades while minimising false positives in untested blades due to greyish tone spots of the abrasive coating matrix and reflected light from the grits.

To ensure a representative range of material pick-up, extending from negligible to near-total coverage, a total of 8 blade-liner pairs (TBT429 tipped blades and MAS abradable liners) were tested under various incursion rate conditions. Specific test parameters are omitted, as the scope of this study focuses on the methodological validation rather than the specific wear mechanics of the test conditions.

The sensitivity analysis was performed on the dataset obtained from these 8 pairs. This analysis identified an optimal threshold value of 0.63, which yielded reliable pick-up ratio results (Figure 12) and was validated via visual inspection of high-resolution images (Figure 11a) and detection maps (Figure 11b) for each blade. Quantitatively, this threshold introduces a systematic error (false positive rate) corresponding to a mean area fraction of 0.0113 ± 0.0019 on untested blades. While this error is inherently present in tested blades, it cannot be isolated from actual material pick-up, as grit facet orientations evolve during testing and their influence on light reflection remains unpredictable.

Table 1
Example of the values provided by the two proposed methodologies for a blade analysed before and after being tested.

Blade condition	Grit density [grit/mm^2]	Volume above matrix level [mm^3/mm^2]	Void density [void/mm^2]	Volume below matrix level [mm^3/mm^2]
Untested	12.17	$2.92{\cdot}10^{-2}$	0.09	$6.13{\cdot}10^{-4}$
Tested	8.75	$2.07{\cdot}10^{-2}$	1.76	$20.74{\cdot}10^{-4}$

3. Results

To validate the tool, the parameters derived from the two developed methods, volume evaluation and feature detection, were used to quantify wear or remaining cutting capability in a set of six blades.

In the volume evaluation approach, parameters include the volume both above and below the matrix level per area. In the feature detection approach, parameters include grit density and void density.

These parameters were assessed for each blade both before and after testing under identical conditions described in the Methodology. The purpose of presenting this data is to demonstrate the application of the proposed method, rather than to directly interpret the underlying mechanisms of blade wear under those conditions.

When blades are tested, grits experience different types of wear, as described in the Introduction, that either shatter and reduce their size, become dulled, or dislodge. As shown in Table 1, these result in a reduction of both its grit density and the volume above the matrix level. Likewise, the appearance of craters as a result of pull-outs during testing is reflected in the increase in void density and volume below matrix level parameters.

All tested blades suffered a reduction of both grits and volume above the matrix level as well as an increase of both voids and volume below the matrix level when tested (Table 1). Whereas the change in the grit density and volume above the matrix level parameters when tested follow very similar trends and show a dependency with the initial value as illustrated in Figures 13a and 13b respectively, the relationship between void density and volume below the matrix level looks more disparate (Figures 13c and 13d) when comparing blade to blade.

Considering these results, it is of further interest to cross-plot the developed parameters to account for initial condition. When blades are manufactured under the same process and come from the same batch, the initial grit density parameter has a direct relationship with the volume above the matrix level per area parameter as seen in the untested blade representation in Figure 14. This indicates that the grits deposited during the manufacturing process exhibit a uniform protruding height regardless of the grit density, which ranges from 9 to 16 grit/mm^2 for the set of blades analysed.

In tested blades, grit wear leads to a reduction in both the volume above the matrix level and the grit density, as shown in the data points of tested blades in Figure 14. As in the untested condition, these two parameters remain linearly correlated when blades are tested under the same conditions. Moreover, the volume lost during testing also exhibits a linear correlation with the initial grit density (untested condition), with the lost volume being 0.312 ± 0.063 of the initial volume regardless of the initial grit density over the 6 blades tested at the same condition. Further investigation is needed to verify these findings using a larger dataset and to evaluate the potential dependency on test conditions.

Regarding the voids left behind by the grit pull-outs, both void density and volume below the matrix level per area undergo an increase subsequent to testing as confirmed in Table 1 for a given blade. The volume below the matrix level per area can be equivalently correlated to the void density, as seen in Figure 15 for the same set of tested blades. Exploring this result further, the volume below the matrix level also correlates quite closely with void density as seen in the Pearson correlation coefficient in Figure 15 ($r = 0.940$), as the volume above the matrix level did with grit density ($r = 0.922$).

Finally, the measured volumes above and below the matrix level may be affected if the blades accumulate significant amounts of abradable material during testing. Although the current version of the image-processing tool cannot isolate or quantify the volume of material adhered to the blade tip, it does reports the affected coating area impacted by this phenomenon.

For the set of six blades used in the method validation, Figure 16 material pick-up during testing was found to be negligible and, therefore, does not cause any impact on the proposed wear-assessment parameters.

4. Discussion

For the assessment of the cutting capability and wear of electroplated tipped blades, two different approaches have been employed and ultimately combined due to their interrelationship. The first approach involves calculating the volume above and below the matrix level per area, which requires minimal post-processing to obtain parameters that capture all the different wear mechanisms: attritious wear, microfracture, macrofracture, and pull-out; all mechanisms abrasive grits undergo during a operation. The second parameter is the active grit density and void density, which require more significant post-processing and does not account for localised grit wear, such as microfracture and attritious wear, but provides a more comprehensive parameter.

To establish a baseline for comparison, it is essential to examine untested blades. Figure 14 shows a correlation between the volume above the matrix level per area and grit density parameters. This correlation has also been further confirmed by analysing untested blades from the same manufacturing batch as illustrated in Figure 17. This is due to the fact that the grit size and the level of infill in the

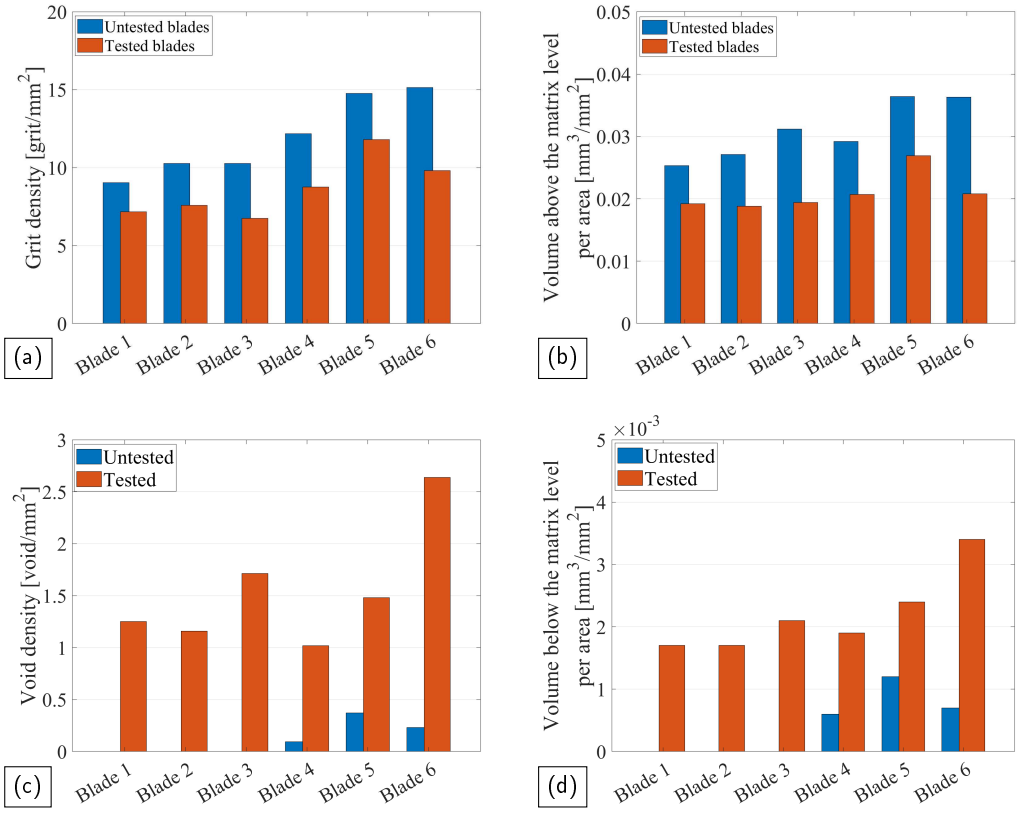

Figure 13: Comparison between the analytical parameters for a set of six blades with different initial grit density: (a) grit density, (b) volume above the matrix level, (c) void density and (d) volume below the matrix level.

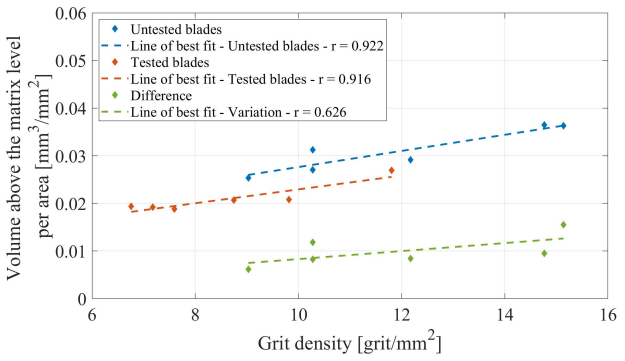

Figure 14: Correlation between the volume above the matrix level per area and grit density for untested and tested blades.

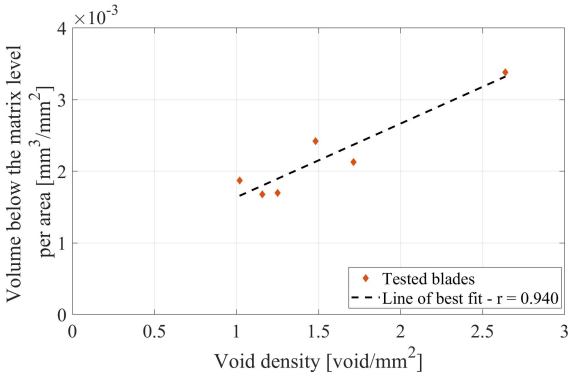

Figure 15: Correlation between the volume below the matrix level per area and void density for tested blades.

matrix follows a homogeneous distribution, and the number of grits per blade is sufficient. Therefore, any of the two proposed parameters can properly describe the blade cutting capability prior to testing. Furthermore, ending in the same result by using two different approaches supports their own validation.

For post-test blade analysis, grit density and volume above the matrix level slightly differ. Figure 14 helps to demonstrate how the different wear mechanisms influence this correlation. While grit density only reflects macrofracture and pull-out of active grits, the volume above the matrix level per area additionally accounts for localised damage caused by microfracture and attritious wear.

The similar gradients but vertical offset between the best-fit lines suggest that all wear mechanisms (microfracture, macrofracture, pull-out, and attritious wear) occur simultaneously. This is consistent with microscopic observations reported in [20]. If only microfracture and attritious wear

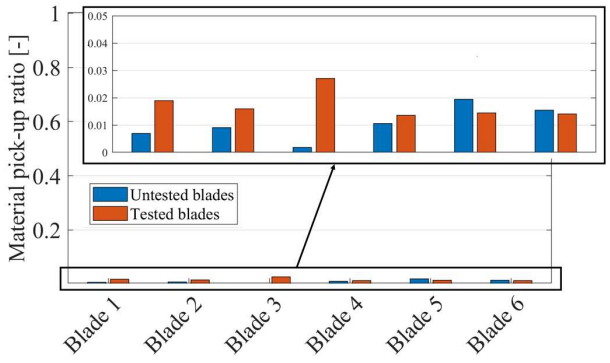

Figure 16: Comparison of the apparent material pick-up for the original set of blades employed to develop the presented methodologies.

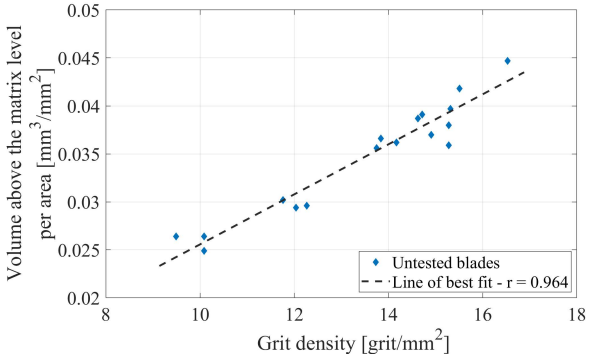

Figure 17: Correlation between the volume above the matrix level per area and grit density for untested blades for further cases.

were present, grit density would remain constant while volume decreased, resulting in vertical displacement of the data points. Conversely, if only macrofracture or pull-out occurred, the data would shift leftward along a single line. This plotting approach therefore helps reveal the combined influence of multiple wear mechanisms during abradable incursion testing.

It is also noteworthy that the difference in volume between the untested and tested condition, or volume removed, as seen in Figure 14 (green line) follows the same trend; it remains almost invariant when plotted against the initial grit density. This suggests that volumetric wear is independent of blade grit density for the considered test condition. However, both the "tested blades" and "variation" lines of best fit may differ from these if testing under different conditions.

Therefore, when it comes to tested blades, measuring volumes above or below the matrix provides a more robust parameter, as it contemplates all the wear mechanisms that produce damage on the grits as opposed to the grit density parameter which misses microfracture and attritious wear. The same justification applies to the voids on tested blades, where the volume below the matrix level per area parameter

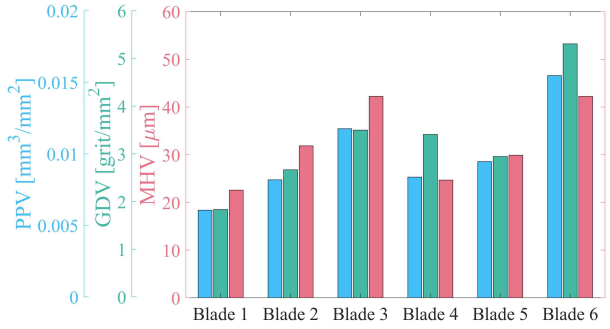

Figure 18: PVV, GDV and MHV parameters for the set of the six blades.

r	PVV	GDV	MHV
PVV	1.000		
GDV	0.950	1.000	
MHV	0.893	0.745	1.000

Table 2
Matrix with the Pearson correlation coefficient (r) between the different parameters that measure the wear produced on blades.

not only takes into consideration that voids have been generated during a test, but it also provides information about the size of the crater left behind. Highly protruding grits require lower forces to be removed as their anchoring is not as firm when compared to a grit deeply embedded into the matrix [26]. Hence, bigger craters leading to larger volumes indicate that the blade went through a harsher contact, a phenomenon that is not considered in the void density parameter.

That said, the main limitation of using volumes as assessment parameters arises when the blade suffers from severe material pick-up. In such cases, two simultaneous and inseparable phenomena occur: a volume reduction due to grit wear, and a volume increase caused by material trapped around the grits, as seen in Figure 11.

Two possible approaches can be considered in this scenario. The first treats the picked-up material as part of the matrix during parameter processing. This interpretation leads to an increase in Sa, a decrease in the positive volume above the matrix, and thus a reduction in the estimated remaining cutting capability of the blade. The second approach relies on the grit density parameter as a preferred indicator, as it accounts for both main sources of volume loss. However, it does not capture localised wear at individual grits as described above. Further testing and analysis is required to understand the impact of heavy material pick-up on these parameters. Additionally, further exploration by elemental analysis, such as EDS, will be considered in future work to validate the proposed methodology of greyscale detection and threshold.

Finally, the established approach of measuring Mean Height Variation (MHV) of a blade during a test, commonly used to quantify damage on bare blades during incursion testing [10], is applied here to the same abrasive-tipped

blades used in this study, which did not exhibit significant material pick-up. The results are then compared with those obtained using the newly developed volume above the matrix level and grit density metrics. To facilitate a direct comparison, Figure 18 presents the variation of these parameters during testing: Grit Density Variation (GDV) and Positive Volume per area Variation (PVV). Crucially, PVV quantifies only regions above the matrix plane, which serves as an invariant reference between the untested and tested blade conditions.

Although Figure 18 suggests similar trends among the three parameters, Table 2, which presents the pairwise Pearson correlation coefficients, reveals notable differences. PVV, which conceptually accounts for the material loss resulting from all types of grit wear mechanisms, exhibits a strong correlation with GDV ($r = 0.950$), which accounts for the two dominant volume-loss-related wear mechanisms, macrofracture and pull-out. A slightly lower correlation is found between PVV and MHV ($r = 0.893$), which lacks a direct conceptual definition within the wear mechanism framework but measures the overall blade height reduction.

On the other hand, the correlation between GDV and MHV is comparatively weaker ($r = 0.745$). This reduced correlation can be attributed to the limited range of wear mechanisms captured by the former, and to the fact that the latter explicitly omits these mechanisms, as they are obscured by the projection of grit particles located in front of or behind these wear events. As a result, PVV is considered the most reliable indicator of overall material loss, particularly when material pick-up is not significant.

5. Conclusion

Conventional techniques used for bare blades are inadequate for abrasive tipped blades due to their complex behaviour and the presence of multiple wear mechanisms. This has motivated the development of a MATLAB-based analytical procedure for evaluating electroplated tipped blades in abradable tests, providing a valuable tool for assessing their cutting capability and wear.

The procedure offers two distinct approaches. The first approach evaluates the volume above and below the matrix level. The second uses a more complex procedure to count the number of grits and voids per area. When examining untested blades, both parameters show a high correlation, indicating their effectiveness in describing cutting capability prior to testing.

For tested blades, measuring volumes above and below the matrix provides a more reliable parameter, considering the microfracture and attritious wear mechanisms which are missed in the grit density parameter. Regarding the void formation, the volume below the matrix level per area parameter offers insights into crater size and embedding of grits, while the void density parameter provides a number of occurrences but fails to capture their severity.

However, using volumes as measurement parameters has limitations when severe material pick-up occurs. In such cases, two different approaches can be considered. The first approach treats the trapped material as an elevation of the matrix level during testing, leading to an apparent volume loss of active grits. The second uses grit density as the main parameter, which accounts for the overall material loss but overlooks localised wear not captured by this metric.

In conclusion, the developed MATLAB-based analytical procedure offers an efficient and automated tool for evaluating the cutting capability and wear of electroplated tipped blades. This overcomes the time constraints of previous studies [26, 20], which relied on manual visual inspection and feature enumeration from micrographs. By accounting for all relevant wear mechanisms and accommodating large test batches, requiring only 2D and 3D data obtainable from a single instrument, it facilitates statistically characterization of blade behaviour under specific test conditions and establishes a foundation for subsequent studies. Furthermore, the developed methods are scalable for application to real gas turbine blades, provided the current rectangular regions of interest (ROIs) are adapted to accommodate complex geometries and the curvature of the abrasive coating matrix.

Acknowledgements

This document is the result of a research project funded by Rolls-Royce Plc.

References

[1] John K Whalen, Eduardo Ed Alvarez, and Lester P Palliser. Thermoplastic labyrinth seals for centrifugal compressors. In *33rd Turbomachinery Symposium*, 2004.

[2] Scott B. Lattime and Bruce M. Steinetz. Turbine engine clearance control systems: Current practices and future directions. *38th AIAA/ASME/SAE/ASEE Joint Propulsion Conference and Exhibit*, (July), 2002.

[3] Raymond E. Chupp, Robert C. Hendricks, Scott B. Lattime, and Bruce M. Steinetz. Sealing in turbomachinery. *Journal of Propulsion and Power*, 22(2):313–349, 2006.

[4] Dieter Sporer, Scott Wilson, and Mitchell Dorfman. *Ceramics for abradable shroud seal applications. Advanced Ceramic Coatings and Interfaces IV symposium proceedings*. 2009.

[5] Dieter Sporer, Scott Wilson, and Mitchell Dorfman. Ceramics for abradable shroud seal applications. pages 39–54, 2009.

[6] Susanne Gebhard, Dan Roth-fagaraseanu, Tanja Wobst, and Matthew Hancock. Advanced coating systems for future shroudless turbines. (2):1–7, 2013.

[7] Matthew Hancock. Shroudless Turbine Sealing, 2019.

[8] Y. D. Liu, J. P. Zhang, Z. L. Pei, J. H. Liu, W. H. Li, J. Gong, and C. Sun. Investigation on high-speed rubbing behavior between abrasive coatings and Al/hBN abradable seal coatings. *Wear*, 456-457:203389, sep 2020.

[9] Andreas Hadjisoteriou. *Investigation of material removal mechanism and thermal response of compressor abradable materials The University of She eld.* PhD thesis, 2021.

[10] Eldar Rahimov, Michael Watson, Andreas Hadjisoteriou, and Matthew Marshall. Investigation of wear mechanisms in AlSi-polyester abradable - Ti(6Al4V) blade contacts using stroboscopic imaging. *Wear*, 494-495, apr 2021.

[11] Bi Wu, Siyang Gao, Ronglu Zhang, Weihai Xue, Shu Li, and Deli Duan. Investigation of the Al-adhesive transfer mechanism on Ti6Al4V blade tips under high-speed rubbing in an aero-turbine engine. *Engineering Failure Analysis*, 142:106692, dec 2022.

[12] Shuai Yang, Siyang Gao, Weihai Xue, Bi Wu, and Deli Duan. Achieving exceptional ultra-high-speed rubbing resistance in NiAlTa/cBN composites through precise structural and compositional design. *Journal of Materials Science & Technology*, 258:187–196, jul 2026.

[13] Michael Watson and Matthew Marshall. Wear mechanisms at the blade tip seal interface. *Wear*, 404-405(March):176–193, 2018.

[14] Rolls-Royce. Rolls-Royce plc internal reports, 2022.

[15] Z. Shi and S. Malkin. Wear of electroplated CBN grinding wheels. *Journal of Manufacturing Science and Engineering, Transactions of the ASME*, 128(1):110–118, 2006.

[16] Wenfeng Ding, Barbara Linke, Yejun Zhu, Zheng Li, Yucan Fu, Honghua Su, and Jiuhua Xu. Review on monolayer CBN superabrasive wheels for grinding metallic materials. *Chinese Journal of Aeronautics*, 30(1):109–134, 2016.

[17] Kai Ding, Yucan Fu, Honghua Su, Xiaobei Gong, and Keqin Wu. Wear of diamond grinding wheel in ultrasonic vibration-assisted grinding of silicon carbide. *International Journal of Advanced Manufacturing Technology*, 71(9-12):1929–1938, 2014.

[18] Surajit Purkayastha. *Mechanical behaviour of c-BN tipped turbine blades*. PhD thesis, 2016.

[19] N. Fois, J. Stringer, and M. B. Marshall. Adhesive transfer in aero-engine abradable linings contact. *Wear*, 304(1-2):202–210, 2013.

[20] M. Watson, N. Fois, and M.B. Marshall. Effects of blade surface treatments in tip–shroud abradable contacts. *Wear*, 338-339:268–281, sep 2015.

[21] Praxair Surface Technologies. Tribomet Abrasive Coatings. page 10372, 2010.

[22] Canan U. Hardwicke and Yuk Chiu Lau. Advances in thermal spray coatings for gas turbines and energy generation: A review. *Journal of Thermal Spray Technology*, 22(5):564–576, 2013.

[23] D. Liu, M. Seraffon, P. E.J. Flewitt, N. J. Simms, J. R. Nicholls, and D. S. Rickerby. Effect of substrate curvature on residual stresses and failure modes of an air plasma sprayed thermal barrier coating system. *Journal of the European Ceramic Society*, 2013.

[24] Svenja Ebert, Robert Mücke, Daniel Mack, Robert Vaßen, Detlev Stöver, Tanja Wobst, and Susanne Gebhard. Failure mechanisms of magnesia alumina spinel abradable coatings under thermal cyclic loading. *Journal of the European Ceramic Society*, 33(15-16):3335–3343, dec 2013.

[25] Radiocommunication Sector International Telecommunication Union. Recommendation ITU-R BT.601-7: Studio encoding parameters of digital television, 2011.

[26] J. R. Davenport, L. Mendez-Garcia, S. Purkayastha, M. E. Hancock, R. J. Stearn, and W. J. Clegg. Material needs for turbine sealing at high temperature. *Materials Science and Technology (United Kingdom)*, 30(15):1877–1883, 2014.